Bioorganic & Medicinal Chemistry Letters 19 (2009) 4724–4728

Contents lists available at ScienceDirect

Bioorganic & Medicinal Chemistry Letters

journal homepage: www.elsevier.com/locate/bmcl

Part 1: Structure–Activity Relationship (SAR) investigations of fused pyrazoles as potent, selective and orally available inhibitors of p38α mitogen-activated protein kinase

Ryan P. Wurz [a,*], Liping H. Pettus [a], Shimin Xu [a], Bradley Henkle [b], Lisa Sherman [b], Matthew Plant [b], Kent Miner [b], Helen McBride [b], Lu Min Wong [b], Christiaan J. M. Saris [b], Matthew R. Lee [c], Samer Chmait [c], Christopher Mohr [c], Faye Hsieh [d], Andrew S. Tasker [a]

[a] Department of Chemistry Research & Discovery, Amgen Inc., One Amgen Center Drive, Thousand Oaks, CA 91320, USA
[b] Department of Inflammation, Amgen Inc., One Amgen Center Drive, Thousand Oaks, CA 91320, USA
[c] Department of Molecular Structure, Amgen Inc., One Amgen Center Drive, Thousand Oaks, CA 91320, USA
[d] Department of Pharmacokinetics and Drug Metabolism, Amgen Inc., One Amgen Center Drive, Thousand Oaks, CA 91320, USA

ARTICLE INFO

Article history:
Received 20 May 2009
Revised 11 June 2009
Accepted 15 June 2009
Available online 17 June 2009

Keywords:
p38
MAP kinase
TNF
Pyrazolopyridinone

ABSTRACT

A novel class of fused pyrazole-derived inhibitors of p38α mitogen-activated protein kinase (MAPK) is disclosed. These inhibitors were evaluated for their ability to inhibit the p38α enzyme, the secretion of TNFα in a LPS-challenged THP1 cell line and TNFα-induced production of IL-8 in 50% human whole blood. This series was optimized through a SAR investigation to provide inhibitors with IC_{50} values in the low single-digit nanomolar range in whole blood. Further investigation of their pharmacokinetic profiles led to the identification of two potent and orally bioavailable p38 inhibitors **10m** and **10q**. Inhibitor **10m** was found to be efficacious *in vivo* in the inhibition of TNFα production in LPS-stimulated Lewis rats with an ED_{50} of 0.1 mg/kg while **10q** was found to have an ED_{50} of 0.05–0.07 mg/kg.

Rheumatoid arthritis (RA) is a chronic and systemic inflammatory disease characterized by inflammation and progressive joint deterioration. Recently, biologics such as Enbrel® (etanercept), Remicade® (infliximab), Humira® (adalimumab), and Kineret® (anakinra) have demonstrated clinical efficacy in the treatment of RA.[1] These protein therapeutics act by blocking the action of TNFα or IL-1 and are significant therapeutic advances for the treatment of these often debilitating conditions.

The development of orally active small molecule inhibitors to modify the proinflammatory cytokine release associated with RA represents an attractive alternative due to drawbacks related to patient cost, and administration associated with biologics.[2] p38 mitogen-activated protein kinase (MAPK) is a member of the intracellular family of MAP kinases implicated in the phosphorylation cascade leading to the release of TNFα and other cytokines including interleukin-1beta (IL-1β), interleukin-6 (IL-6) and interleukin-8 (IL-8). p38 kinases are activated by a variety of stress stimuli including osmotic shock, ionizing radiation, mechanical wear, and cytokine stimulation.[3] Activation results in the release of TNFα among other cytokines and the migration of white blood cells to the site of inflammation.

p38 exists in four isoforms (α, β, γ, and δ) and expression of each isoform varies among different cell types of the immune system. The p38α isoform is believed to be the most clinically relevant for the treatment of RA,[4] hence, p38α has emerged as an attractive target for small molecule drug discovery to blockade the action of TNFα.[5]

Amgen recently disclosed a series of phthalazine-derived p38 inhibitors[6] which were found to be highly potent in cell-based assays and efficacious in the rat collagen induced arthritis (CIA) model. Although these inhibitors exhibited exceptional selectivity for p38αβ over other kinases, the future goal of the program was to further improve upon this selectivity in addition to reducing brain exposure (data not shown). Herein, the discovery and exploratory structure–activity relationship (SAR) study of a novel pyrazolopyridinone chemotype (**1**) is described (Fig. 1).

Inspiration for this scaffold was based on recent reports of p38 inhibitors containing a benzamide unit linked to a heterocycle via an aniline nitrogen (Fig. 2). The first of these reports contained a benzamide tethered to a triazine scaffold (**2**, Fig. 2).[7] In subsequent disclosures, the triazine moiety was replaced with various other heteroaromatic groups including 5-cyanopyrimidines (**3**),[8]

* Corresponding author. Tel.: +1 805 313 5400; fax: +1 805 480 1337.
E-mail address: rwurz@amgen.com (R.P. Wurz).

0960-894X/$ - see front matter © 2009 Elsevier Ltd. All rights reserved.
doi:10.1016/j.bmcl.2009.06.058

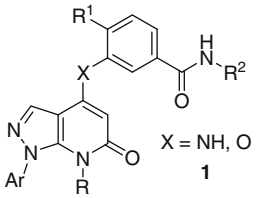

Figure 1. Pyrazolopyridinone-derived p38 inhibitors.

4-(phenylamino)-pyrrolo[2,1-*f*][1,2,4] triazines (**4**)[9] and more recently pyrazolopyrimidines (**5**).[10]

The compounds necessary for our SAR investigation were prepared in seven steps via the general route illustrated in Scheme 1. Thus, suitably functionalized pyrazoles (**6**) were readily prepared in excellent yields (70–99%) upon treatment of an aryl hydrazine with ethyl (ethoxymethylene) cyanoacetate.[11] Amine bis(acetylation) followed by mono-deprotection using ethanolic potassium hydroxide at room temperature afforded the 5-aminopyrazole monoacetate (**7**) which could be N-alkylated using the desired halide (R^1X) (33–82% yield over three steps).[12] A variety of bases[13] were then examined for the construction of the pyridinone ring through an intramolecular cyclization. Ultimately, lithium diisopropyl amide (LDA) was found to be the most effective base to achieve this cyclization (35–99%). Chlorination of the 4-hydroxypyridinone cyclization product using phosphorus oxychloride[14] furnished the common chloride coupling partner in modest yields (**9**, 23–75%). Subsequent Buchwald–Hartwig amination with the desired aniline afforded analogues **10** (X = NH) in moderate yields (15–87%)[15] while Buchwald etherification with phenols yielded the corresponding ether analogues **10** (X = O) in low to moderate yields (20–60%).[16]

The preliminary SAR focused on optimization of R^2. The compounds were tested for their ability to inhibit p38α (by monitoring the phosphorylation of ATF2), as well as their potency in lipopolysaccharide (LPS) challenged TNFα production in a THP1 cell line and in TNFα stimulated IL-8 secretion in 50% human whole blood (hWB, Table 1).[17]

Compounds with R^2 groups such as tetrahydropyran (**10a**) or fluorinated aryl groups (**10b–c**) were inactive against p38α. Introduction of a 3-substituted-4-methyl-pyridine motif at R^2 (**10d**) resulted in weak inhibition of p38α. Incorporation of an *ortho*-tolyl benzamide as R^2 provided several compounds which were potent inhibitors of p38α and exhibited IC_{50} values in the low single-digit

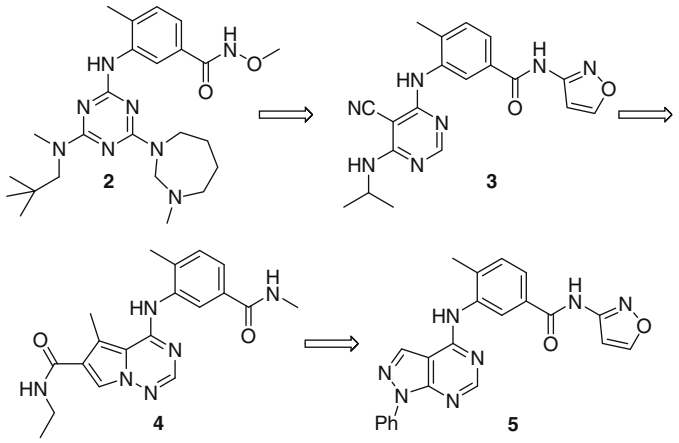

Figure 2. Examples of Bristol-Myers Squibb p38 inhibitors containing an aniline N-linked benzamide motif.

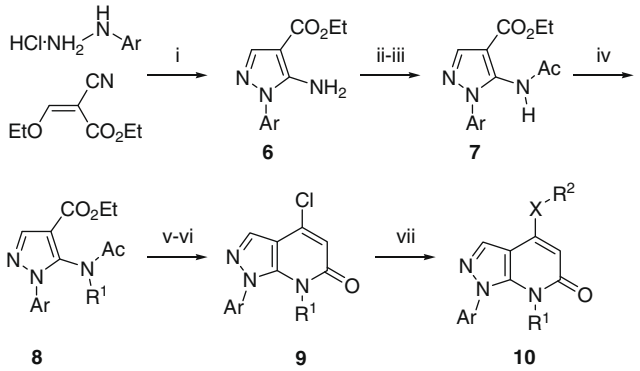

Scheme 1. General synthetic route used to access aniline NH- and O-linked pyrazolopyridinone benzamides. Reagents and conditions: (i) Et_3N, EtOH, 90 °C; (ii) Ac_2O, DMAP, Et_3N, 1,2-DCE, reflux; (iii) KOH, EtOH, rt; (iv) NaH, LiBr, R^1X, 10:1 DME:DMF; (v) LDA, THF, −78 °C to rt; (vi) $POCl_3$, 100 °C; (vii) X = NH: $Pd_2(dba)_3$, Dave-Phos, R^2NH_2, LiHMDS, THF, 60 °C; X = O: $Pd_2(dba)_3$, *t*-Bu_2X-Phos, R^2OH, K_3PO_4, PhMe:THF 5:1, μwave, 120 °C.

nanomolar range in hWB (**10e–h**). The sterically demanding *tert*-butyl amide (**10i**) exhibited a 100-fold reduction in potency in the TNFα/IL-8 assay in hWB compared to the cyclopropyl amide analogue **10h**. Replacement of the amide with a carboxylic acid (**10j**) led to loss of enzyme and cell-based potency, illustrating the importance of the amide in this position.

SAR was then directed to further optimization of the scaffold while conserving the cyclopropylamide[18] portion of the benzamide motif (Table 2). The fluorine substitution pattern on the aryl group at the N-1 position of the pyrazolopyridinone ring had little influence on IC_{50} values in hWB, varying from 1.3–2.5 nM across a series (e.g., **10k**,**h**,**u**,**y**). Replacement of the benzamide *ortho*-tolyl group (R^3 = Me) with an *ortho*-chloro group (R^3 = Cl) also resulted in potent compounds (e.g., **10m**,**q**,**v**,**z**). In contrast, introduction of a fluorine atom (R^3 = F) at this position resulted in a >4-fold reduction in hWB potency (e.g., **10s**,**aa**) as compared to R^3 = Me. Modifying the R^1-substituent from a methyl group to an ethyl group was well tolerated (e.g., **10n–p**,**r**).[19]

Replacement of X = NH to X = O generally resulted in a sizable erosion in THP1 and hWB potency. This is possibly attributed to the decline in solubility of these compounds.[20] One exception to this trend was compound **10ab** which retained low single-digit nanomolar potency in the cellular assays.

In light of their excellent cellular potencies, a series of compounds were profiled for their pharmacokinetic (PK) parameters in order to differentiate these compounds for further studies (Table 3). With the exception of compounds **10g** and **10z**, all of the compounds demonstrated low to moderate clearance. However, compounds **10m** and **10q** stood apart as they displayed good exposure (*AUC*) and excellent oral bioavailability (*%F*) following oral dosing at 2 mg/kg.

The X-ray co-crystal structure of **10h** bound to unphosphorylated p38α (Fig. 3)[21] revealed several key binding interactions. The NH of the Met109 linker residue engages in a hydrogen bonding interaction with N-2 of the pyrazolopyridinone scaffold (3.2 Å) while the N-1 aryl group is projected into a hydrophobic pocket near the hinge region of the p38α enzyme. This aryl group is skewed with respect to the pyrazolopyridinone scaffold as previously reported.[10] The floor of this hydrophobic pocket contains an Ala157 residue, which is smaller than the corresponding residue in over 98% of the kinome.[22] This residue engages in a tight van der Waals contact with the 2-fluorophenyl substituent (3.4 Å), thereby providing a structure-based approach for enhancing selectivity over other kinases. The 'gate-keeper' residue, Thr106, is internally

Table 1
SAR of modifications to Ar and R[2][a]

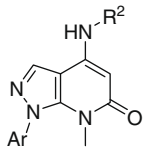

10

Compd	Ar	R^2	p38α IC_{50} (nM)	THP1 LPS/TNFα IC_{50} (nM)	hWB TNFα/IL-8 IC_{50} (nM)
10a	3-F-Ph	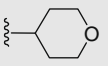	>1000	>2500	>2500
10b	2,6-Di-F-Ph	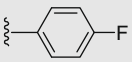	>1000[b]	546[b]	>833
10c	2,4-Di-F-Ph	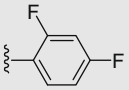	>1000[b]	937[b]	>2500
10d	2,5-Di-F-Ph	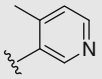	444[b]	208[b]	403
10e	2,4-Di-F-Ph	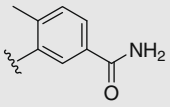	2.6[b]	1.9	3.4
10f	2,5-Di-F-Ph	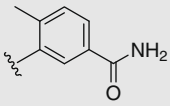	3.7[b]	7.5	7.1
10g	2,4-Di-F-Ph	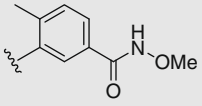	1.1	1.1	1.4
10h	2,4-Di-F-Ph	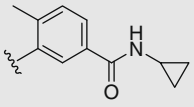	3.2[b]	1.0	2.4
10i	2,4-Di-F-Ph	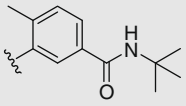	269[b]	65[b]	204
10j	2,4-Di-F-Ph	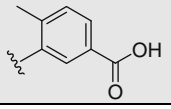	>1000	>2500[b]	>2500

[a] The IC_{50} data are mean values derived from at least three independent dose–response curves. Variability around the mean value was <50%.
[b] Data represents an average of two dose–response curves.

hydrogen-bonded to the carbonyl of His107 while the oxygen lone pair participates in a hydrogen bond with the aniline NH (3.0 Å). The cyclopropyl amide forms two key interactions with Asp168 and Glu71. The amide carbonyl forms a hydrogen bond to the NH of Asp168 (2.9 Å) while the carboxylate of Glu71 forms a hydrogen bond with the NH of the cyclopropyl amide (3.0 Å). Another feature of the binding of this inhibitor is the presence of two water molecules which serve to bridge the pyridinone carbonyl to the carboxylate of Asp168 and Lys53 through a network of hydrogen bonds. The 'DFG in' configuration (residues Asp168, Phe169, Gly170) is observed as expected.[23]

Compounds **10m** and **10q** were screened against a panel of 60 kinases for potential off-target liabilities.[24] While compound **10m** showed no selectivity over p38β (IC_{50} = 4 nM), it was very selective against p38γ, p38δ isoforms and JNK1-3 (IC_{50} values >10 μM). It also showed some inhibitory activity against c-Raf (40% POC at

Table 2
SAR of modifications to R^1, R^3 and Ar[a]

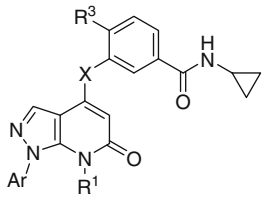

10

Compd	Ar	R^1	R^3	X	p38α IC_{50} (nM)	THP1 LPS/TNFα IC_{50} (nM)	hWB TNFα/IL-8 IC_{50} (nM)
10k	3-F-Ph	Me	Me	NH	3.3[b]	1.3	1.7
10l	3-F-Ph	Me	Me	O	8.5	12	29
10m	4-F-Ph	Me	Cl	NH	1.5	1.1	2.5
10n	4-F-Ph	Et	Me	NH	4.0[b]	1.1	1.9
10o	4-F-Ph	Et	Cl	NH	1.2	1.0	0.93
10p	4-F-Ph	Et	Me	O	4.0	1.8	13
10h	2,4-Di-F-Ph	Me	Me	NH	3.2[b]	1.0	2.4
10q	2,4-Di-F-Ph	Me	Cl	NH	1.0	0.44	1.1
10r	2,4-Di-F-Ph	Et	Cl	NH	1.1	0.67	1.3
10s	2,4-Di-F-Ph	Me	F	NH	13[b]	6.7	19
10t	2,4-Di-F-Ph	Me	Me	O	7.8[b]	3.5	16
10u	2,5-Di-F-Ph	Me	Me	NH	2.9[b]	1.0	2.5
10v	2,5-Di-F-Ph	Me	Cl	NH	1.1	1.1	1.9
10w	2,5-Di-F-Ph	Me	Me	O	6.1[b]	5.0	16
10x	2,5-Di-F-Ph	Me	Cl	O	3.3[b]	14	79
10y	2,6-Di-F-Ph	Me	Me	NH	1.9[b]	0.87	1.3
10z	2,6-Di-F-Ph	Me	Cl	NH	1.1[b]	0.62	1.5
10aa	2,6-Di-F-Ph	Me	F	NH	1.9	3.2	8.2
10ab	2,6-Di-F-Ph	Me	Me	O	1.4	1.0	2.6

[a] The IC_{50} data are mean values derived from at least three independent dose–response curves. Variability around the mean value was <50%.
[b] Data represents an average of two dose–response curves.

Table 3
Mean pharmacokinetic parameters for a series of compounds in male Sprague–Dawley rats[a]

Compd	iv (2.0 mg/kg in DMSO)			po (2.0 mg/kg)[b]	
	CL ((L/h)/kg)	V_{dss} (L/kg)	$t_{1/2}$ (H)	$AUC_{(0\text{-inf.})}$ (ng.h/mL)	F (%)
10g	2.6	1.7	3.3	120	15
10m	0.26	0.97	5.8	6547	84
10o	0.41	1.8	3.7	2293	45
10p	0.27	1.1	3.2	1496	41
10q	0.37	1.2	3.8	4612	81
10r	0.42	1.5	3.4	776	16
10v	0.52	1.2	2.1	2163	56
10y	0.88	1.2	2.8	273	12
10z	1.3	1.9	3.4	139	9
10ab	0.63	1.3	2.3	244	7

[a] Values are for an average of three rats.
[b] Vehicle: 1% Pluronic F68, 1% HPMC, 15% hydroxypropyl β-cyclodextrin, 83% water.

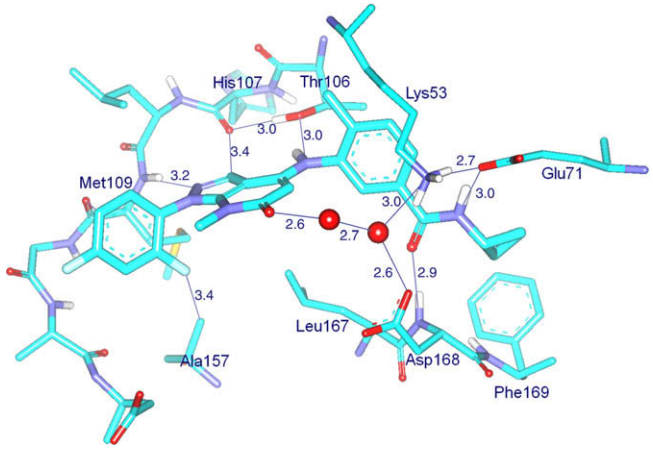

Figure 3. X-ray co-crystal structure of compound **10h** with unphosphorylated p38α.

1.5 μM). Compound **10q** displayed a very similar selectivity profile to that of **10m** (c-Raf 75% POC at 1.5 μM). Compound **10m** was 97% and 94% bound to rat and human plasma protein, respectively (determined by ultrafiltration methods) while compound **10q** was 98% and 96% bound to rat and human plasma protein, respectively. Compound **10m** showed little inhibition of CYP 450 isoforms with 3A4 and 1A2 (IC_{50} >30 μM) and 2C9, 2C19 and 2D6 (IC_{50} >21 μM). Compound **10q** did have a CYP 450 liability with 2C9 (IC_{50} 8.4 μM). Two other isoforms were tested and found to be satisfactory with 2C19 (IC_{50} 16 μM), and 2D6 (IC_{50} 22.7 μM).

Based on their suitable PK and selectivity profiles, compounds **10m** and **10q** were advanced to in vivo studies. The in vivo efficacy of compounds **10m** and **10q** were demonstrated in an animal disease model of LPS induced TNFα production in female Lewis rats.[25] Both compounds were administered at 0.01, 0.03, 0.1, and 0.3 mg/kg and resulted in an ED_{50} of ca. 0.1 mg/kg for compound **10m** (Fig. 4) and an ED_{50} of ca. 0.05–0.07 mg/kg for compound **10q** (Fig. 5). The plasma exposure at the ED_{50} is 3.2 ng/mL for compound **10m** and estimated to be between 0.9 and 1.3 ng/mL for compound **10q**. Compounds **10m** and **10q** were also found to have very low brain to plasma ratios of 0.04 and 0.06, respectively.

In conclusion, through SAR studies a novel class of pyrazolopyridinone p38 inhibitors has been identified. Compounds from this series show excellent potency against p38α, in THP1 cell-based assays and in TNFα challenged IL-8 secretion assays in 50% hWB. Pharmacokinetic profiling also revealed that inhibitors **10m** and **10q** were orally bioavailable and displayed low iv clearance. Compounds **10m** and **10q** were evaluated in vivo and found to inhibit

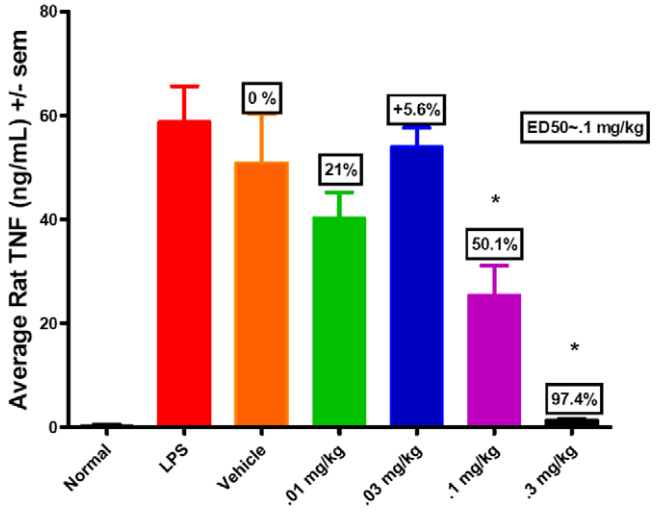

Figure 4. Effect of **10m** on LPS induced TNFα production in female Lewis rats. Vehicle or compound was dosed po 60 min prior to injection with LPS IV (100 μg/rat). Blood was collected 90 min later. Serum TNFα levels were determined by ELISA (Biosource). Data points represent mean ±STE (n = 6 rats/group): (*) p <0.01 versus vehicle control.

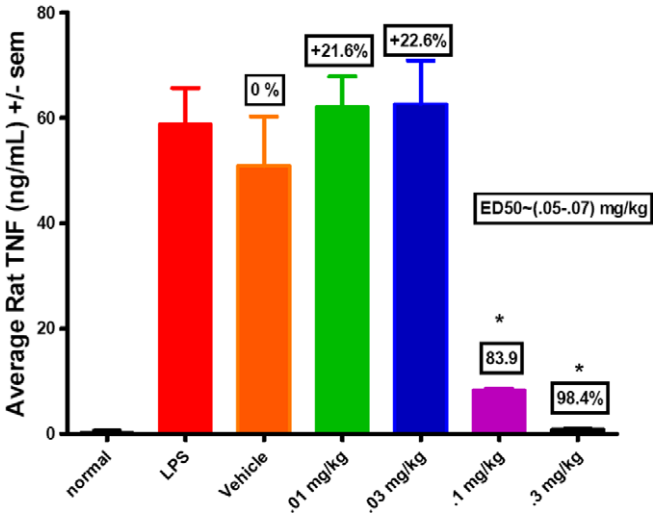

Figure 5. Effect of **10q** on LPS induced TNFα production in female Lewis rats. Vehicle or compound was dosed po 60 min prior to injection with LPS IV (100 μg/rat). Blood was collected 90 min later. Serum TNFα levels were determined by ELISA (Biosource). Data points represent mean ±STE (n = 6 rats/group): (*) p <0.01 versus vehicle control.

the LPS induced production of TNFα with ED_{50}'s of 0.1 mg/kg and ca. 0.05–0.07 mg/kg, respectively.

Acknowledgments

We acknowledge Randall Hungate and Terry Rosen for their support.

References and notes

1. (a) Keystone, E. C. *Rheu. Dis. Clin. North Am.* **2001**, *27*, 427; (b) Seymour, H. E.; Worsley, A.; Smith, J. M.; Thomas, S. H. L. *Br. J. Clin. Pharmacol.* **2001**, *51*, 201; (c) Anon *Physicians' Desk Reference*, 54th ed.; Medical Economics: Montvale, 2000. pp. 927–1413.
2. Stanczyk, J.; Ospelt, C.; Gay, S. *Curr. Opin. Rhe.* **2008**, *20*, 257.
3. (a) Margutti, S.; Laufer, S. A. *ChemMedChem* **2007**, *2*, 1116; (b) Schett, G.; Zwerina, J.; Firestein, G. *Ann. Rhe. Dis.* **2008**, *67*, 909.
4. O'Keefe, S. J.; Mudgett, J. S.; Cupo, S.; Parsons, J. N.; Chartrain, N. A.; Fitzgerald, C.; Chen, S.-L.; Lowitz, K.; Rasa, C.; Visco, D.; Luell, S.; Carballo-Jane, E.; Owens, K.; Zaller, D. M. *J. Biol. Chem.* **2007**, *282*, 34663.
5. For recent reviews on the design of small molecule inhibitors for p38 MAP kinase, see: (a) Pettus, L. H.; Wurz, R. P. *Curr. Top. Med. Chem.* **2008**, *8*, 1452; (b) Wagner, G.; Laufer, S. *Med. Res. Rev.* **2006**, *26*, 1; (c) Westra, J.; Limburg, P. C. *Mini-Rev. Med. Chem.* **2006**, *6*, 867; (d) Dominguez, C.; Tamayo, N.; Zhang, D. *Exp. Opin. Ther. Pat.* **2005**, *15*, 801; (e) Dominguez, C.; Powers, D. A.; Tamayo, N. *Curr. Opin. Drug Dis. Dev.* **2005**, *8*, 421; (f) Lee, M. R.; Dominguez, C. *Curr. Med. Chem.* **2005**, *12*, 763.
6. (a) Herberich, B.; Cao, G.-Q.; Chakrabarti, P. P.; Falsey, J. R.; Pettus, L.; Rzasa, R. M.; Reed, A. B.; Reichelt, A.; Sham, K.; Thaman, M.; Wurz, R. P.; Xu, S.; Zhang, D.; Hsieh, F.; Lee, M. R.; Syed, R.; Li, V.; Grosfeld, D.; Plant, M. H.; Henkle, B.; Sherman, L.; Middleton, S.; Wong, L. M.; Tasker, A. S. *J. Med. Chem.* **2008**, *51*, 6271; (b) Pettus, L. H.; Xu, S.; Cao, G.-Q.; Chakrabarti, P. P.; Rzasa, R. M.; Sham, K.; Wurz, R. P.; Zhang, D.; Middleton, S.; Henkle, B.; Plant, M. H.; Saris, C. J. M.; Sherman, L.; Wong, L. M.; Powers, D. A.; Tudor, Y.; Yu, V.; Lee, M. R.; Syed, R.; Hsieh, F.; Tasker, A. S. *J. Med. Chem.* **2008**, *51*, 6280.
7. Leftheris, K.; Ahmed, G.; Chan, R.; Dyckman, A. J.; Hussain, Z.; Ho, K.; Hynes, J., Jr.; Letourneau, J.; Li, W.; Lin, S.; Metzger, A.; Moriarty, K. J.; Riviello, C.; Shimshock, Y.; Wen, J.; Wityak, J.; Wrobleski, S. T.; Wu, H.; Wu, J.; Desai, M.; Gillooly, K. M.; Lin, T. H.; Loo, D.; McIntyre, K. W.; Pitt, S.; Shen, D. R.; Shuster, D. J.; Zhang, R.; Diller, D.; Doweyko, A.; Sack, J.; Baldwin, J.; Barrish, J.; Dodd, J.; Henderson, I.; Kanner, S.; Schieven, G. L.; Webb, M. *J. Med. Chem.* **2004**, *47*, 6283.
8. Liu, C.; Wrobleski, S. T.; Lin, J.; Ahmed, G.; Metzger, A.; Wityak, J.; Gillooly, K. M.; Shuster, D. J.; McIntyre, K. W.; Pitt, S.; Shen, D. R.; Zhang, R. F.; Zhang, H.; Doweyko, A. M.; Diller, D.; Henderson, I.; Barrish, J. C.; Dodd, J. H.; Schieven, G. L.; Leftheris, K. *J. Med. Chem.* **2005**, *48*, 6261.
9. Hynes, J., Jr.; Dyckman, A. J.; Lin, S.; Wrobleski, S. T.; Wu, H.; Gillooly, K. M.; Kanner, S. B.; Lonial, H.; Loo, D.; McIntyre, K. W.; Pitt, S.; Shen, D. R.; Shuster, D. J.; Yang, X.; Zhang, R.; Behnia, K.; Zhang, H.; Marathe, P. H.; Doweyko, A. M.; Tokarski, J. S.; Sack, J. S.; Pokross, M.; Kiefer, S. E.; Newitt, J. A.; Barrish, J. C.; Dodd, J.; Schieven, G. L.; Leftheris, K. *J. Med. Chem.* **2008**, *51*, 4.
10. Das, J.; Moquin, R. V.; Pitt, S.; Zhang, R.; Shen, D. R.; McIntyre, K. W.; Gillooly, K.; Doweyko, A. M.; Sack, J. S.; Hongjian, Z.; Kiefer, S. E.; Kish, K.; McKinnon, M.; Barrish, J. C.; Dodd, J. H.; Schieven, G. L.; Leftheris, K. *Bioorg. Med. Chem. Lett.* **2008**, *18*, 2652.
11. Goldstein, D. M.; Alfredson, T.; Bertrand, J.; Browner, M. F.; Clifford, K.; Dalrymple, S. A.; Dunn, J.; Freire-Moar, J.; Harris, S.; Labadie, S. S.; La Fargue, J.; Lapierre, J. M.; Larrabee, S.; Li, F.; Papp, E.; McWeeney, D.; Ramesha, C.; Roberts, R.; Rotstein, D.; Pablo, B. S.; Sjogren, E. B.; So, O.-Y.; Talamas, F. X.; Tao, W.; Trejo, A.; Villasenor, A.; Welch, M.; Welch, T.; Weller, P.; Whiteley, P. E.; Young, K.; Zipfel, S. *J. Med. Chem.* **2006**, *49*, 1562.
12. Liu, H.; Ko, S.-B.; Josien, H.; Curran, D. P. *Tetrahedron Lett.* **1995**, *36*, 8917.
13. Other bases such as KO*t*-Bu were found not to promote this cyclization, see: Sherlock, M. H.; Kaminski, J. J.; Tom, W. C.; Lee, J. F.; Wong, S.-C.; Kreutner, W.; Bryant, R. W.; McPhail, A. T. *J. Med. Chem.* **1988**, *31*, 2108.
14. (a) Blackburn, C.; LaMarche, M. J.; Brown, J.; Che, J. L.; Cullis, C. A.; Lai, S.; Maguire, M.; Marsilje, T.; Geddes, B.; Govek, E.; Kadambi, V.; Doherty, C.; Dayton, B.; Brodjian, S.; Marsh, K. C.; Collins, C. A.; Kym, P. R. *Bioorg. Med. Chem. Lett.* **2006**, *16*, 2621; b McCarthy, J. R. WO 98/35967, 1998.
15. Charles, M. D.; Schultz, P.; Buchwald, S. L. *Org. Lett.* **2005**, *7*, 3965.
16. Burgos, C. H.; Barder, T. E.; Huang, X.; Buchwald, S. L. *Angew. Chem., Int. Ed.* **2006**, *45*, 4321.
17. For a description of the experimental details of the biological assays, see: Ref. 6.
18. The cyclopropyl amide was chosen for further optimization due to its favorable PK profile when compared to the methoxy and primary amides.
19. A more extensive SAR investigation surrounding the nature of the aryl group at N-1 and the R^1-substituent will be reported in due course on a related class of pyrazolopyridinone p38 inhibitors, in preparation.
20. The solubility data for compounds **10m**,**q**,**t**,**v**,**x** in 0.01 N HCl were 31.2, 67.1, 5.7, 28.6 and 24.8 μg/mL, respectively, while in phosphate buffer saline they were found to be 26.6, 60.6, 5.3, 24.9, and 14.7 μg/mL, respectively, and in simulated intestinal fluid they were found to be 38.8, 81.7, 12.2, 35.2 and 49.0 μg/mL, respectively.
21. The X-ray coordinates have been deposited in the RCSB Protein Data Bank database (RCSB ID code: RCSB051790 and PDB ID code: 3GFE). We also thank the Advanced Light Source staff at beamline 5.0.2 for their support. The Advanced Light Source is supported by the Director, Office of Science, Office of Basic Energy Sciences, Materials Sciences Division, of the U.S. Department of Energy under Contract DE-AC03-76SF00098 at Lawrence Berkeley National Laboratory.
22. Manning, G.; Whyte, D. B.; Martinez, R.; Hunter, T.; Sudarsanam, S. *Science* **2002**, *298*, 1912.
23. For a leading references and examples on 'DFG in' versus 'DFG out', See: (a) Bukhtiyarova, M.; Karpusas, M.; Northrop, K.; Namboodiri, H. V. M.; Springman, E. B. *Biochemistry* **2007**, *46*, 5687; (b) Angell, R. M.; Angell, T. D.; Bamborough, P.; Bamford, M. J.; Chung, C.-W.; Cockerill, S. G.; Flack, S. S.; Jones, K. L.; Laine, D. I.; Longstaff, T.; Ludbrook, S.; Pearson, R.; Smith, K. J.; Smee, P. A.; Somers, D. O.; Walker, A. L. *Bioorg. Med. Chem. Lett.* **2008**, *18*, 4433.
24. Kinase profiling on all kinases were tested at their apparent K_m of ATP, using 1.5 μM inhibitor. The kinase selectivity panel included p38(α, β, γ, δ), c-KIT, JNK(1,2,3), JAK2, b-RAF, c-RAF, MAPKAPK2, KDR, SYK, RSK1, PI3 K(α,δ), LCK, SRC, Aur(A), c-Met, PIM2, ABL, FYN, LYN, AKT(1,2), CHK(1,2), Erk(1,2), FLT3, GSK3β, ROCK2, PAK2, PKGα, MST2, INSR, MSK1, PKCβ2, CDK2, MARK1, IGF1R, FGFR1, PKACα, PRAK, PKD2, CK1δ, PKCz, TAK1, DYRK1α, CAMK(2,4), AMPK, HGK, p70S6 K, IRAK4, SGK1, BTK, PDGFRβ.
25. Hegen, M.; Keith, J. C., Jr.; Collins, M.; Nickerson-Nutter, C. L. *Ann. Rhe. Dis.* **2008**, *67*, 1505.